ChemElectroChem

Research Article
doi.org/10.1002/celc.202400597

Chemistry Europe
European Chemical Societies Publishing

www.chemelectrochem.org

NaDFOB and FEC as Electrolyte Additives Enabling Improved Cyclability of Sodium Metal Batteries and Sodium Ion Batteries

Zhengqi Wang[a, b] and Andreas Hofmann*[a]

Sodium metal is often considered as an anode material to improve the energy-density of sodium metal batteries (SMB) respectively sodium ion-based batteries (SIB). However, the active Na metal anode is a particular challenge. To formulate a suitable electrolyte has therefore been a key issue to stabilize sodium metal anodes. Here we report additive strategies by using the additives sodium difluoro(oxalato) borate (NaDFOB) or/and fluoroethylene carbonate (FEC) in the baseline electrolyte solution of 1 M $NaPF_6$ in ethylene carbonate/propylene carbonate to overcome these issues. For the SMB with sodium anode and carbon-coated $Na_3V_2(PO_4)_3$ (NVP) cathode, a stable cell cycling up to 600 cycles (capacity retention about 96 ± 3 %) was reached by using only 1–2 wt. % NaDFOB, compared to only less than 75 cycles of the baseline electrolyte. Sodium plating/stripping tests, voltammetry measurements, impedance analysis as well as cell tests were performed in order to reveal the electrochemical characteristics of the electrolytes including additive effects. The optimal SIB cell performance in cells containing hard carbon and NVP was achieved by using 2 wt.-% NaDFOB. NaDFOB electrolyte can be considered as a beneficial additive for Na metal cell and its application could be also extended for full SIBs.

Introduction

The ever-growing demands for low-cost, high-energy density and sustainable energy storage systems require the development of post-lithium battery technologies, including sodium ion-based batteries (SIB) and rechargeable sodium-metal batteries (SMB) due to the natural abundance of Na, the high theoretical specific capacity (1166 mAh g^{-1}) and the low redox potential of −2.71 V vs. standard hydrogen electrode (SHE).[1] Their counterpart, namely Li metal batteries, have already been intensively investigated as a revived anode to achieve high energy density.[2] However, several challenges in developing a reliable sodium metal anode should be encountered, such as dendrite growth, parasitic reactions at the Na anode interface, and volume change, leading to electrolyte consumption, irreversible plating-stripping of sodium and thus battery failure.[1,3]

Forming a desirable solid electrolyte interface (SEI) protective layer at the Na anode interface plays a crucial role for stabilizing the Na anode and improving its cyclability. An effective SEI layer can impede unwanted parasitic electrode reactions (e.g. electrolyte decomposition), control the dendrite growth, limit the volume change and favor the fast ion transport as well as interface reaction kinetics. Additionally, the SEI layer should not dissolve in the electrolyte and remain stable over operating voltage and temperature range.[1,3–6] Normally, the SEI layer on Na metal is formed by two main processes, namely by (1) chemical passivation and (2) electrochemical reactions between the active Na metal interface and the electrolyte.[2,7,8]

The more reactive nature of sodium metal relative to Li determines its higher reactivity towards electrolytes.[4,9] The chemical reaction between sodium metal and electrolyte already occurs when the sodium metal anode is assembled into the cells.[10] The observed reactivity of electrolyte (storage over Na metal) depends severely on the conducting salt and electrolyte solvent..[10,11] Ponrouch's group has compared the interface layers formed on Na, which was immersed in $NaPF_6$-carbonate mixtures and subsequently electrochemically polarized.[8] The results of the infrared (IR) spectroscopy revealed that the formed SEI layer on Na is thicker and there were detected some differences in the species after polarization, compared to those being there only by chemical passivation. Similar to those of the Li metal anode, the formed SEI layer on Na metal anode is strongly dependent on the electrolyte composition and electrochemical condition,[1,4,9] but is usually more unstable when formed in conventional carbonate-based electrolytes[8] than in ether based electrolytes. The failure of the initially formed SEI layer weakens the long-

[a] Dr. Z. Wang, Dr. A. Hofmann
Institute for Applied Materials (IAM),
Karlsruhe Institute of Technology (KIT),
Hermann-von-Helmholtz-Platz 1, 76344 Eggenstein-Leopoldshafen, Germany
Tel.: +49 72160825920
E-mail: andreas.hofmann2@kit.edu

[b] Dr. Z. Wang
Department of Microsystems Engineering
University of Freiburg
Georges-Köhler-Allee 102, Freiburg D-79110, Germany

Supporting information for this article is available on the WWW under https://doi.org/10.1002/celc.202400597

term cyclability of Na anodes, mainly due to the following reasons:

(1) the nonuniform composition of SEI leads to heterogeneity of the ionic deposition and the Na metal anode itself exhibits a larger volumetric change during charge and discharge, compared to carbon-based anode materials.[4,9] Consequently, the mechanical stress cause generation of cracks, which is believed to be the nucleation sites for dendrite growth.[2,12,13] For Na metal, the dendrite growth might cause a typical metal electrode failure because of the subsequent electrolyte depletion and the dendrite's dissolution from the root metal.[13,14]
(2) the characteristics of the SEI itself, i.e. the dissolution of the SEI is a major concern.[15,16] Breakdown of the (partially) soluble SEI leads to a continuous re-formation of SEI during the Na electrode-deposition, which, in turn, worsen the nonuniformity of the SEI.[4,6,16]

Similarly, the cathode-electrolyte interface layer (CEI) formed by the oxidative decomposition of the electrolyte on cathode materials is also facing failure issues regarding to its chemical and electrochemical stability and/or solubility.[6,17,18] However, more studies are needed to reveal the relationship between electrolyte composition, CEI characteristics and cell performances.

To address these issues, the electrolyte design has been proven as an effective possibility to tailor a chemically, mechanically and ion-flux favorable interface layer that enable a stable and long-term Na battery cyclability. These efforts can be roughly concluded as following:

- Using improved electrolyte solvents.[19–22]
- Using selected salt anions to tune inorganic components in the inner SEI part and possibly to affect the thickness and structure of the SEI formed.[3,10,20–31]
- Adopting super-concentrated electrolytes to boost carrier density and suppress free solvent molecules leading to higher voltage stability and elimination of side reactions.[32,33]
- Using various additives, which mainly are inspired by the efforts for Li-metal batteries.[6,24,27,34]

Fluoroethylene carbonate (FEC) is an effective electrolyte additive that significantly improves the cycling stability.[6,34] FEC has a relatively lower LUMO energy compared to other solvents, so it can be preferentially reduced on the anode and thus considered as a film-forming additive.[35] For Na metal anodes, FEC (co-solvent or additives) has shown the ability to suppress solvent decomposition and improve electrochemical performance in carbonate-based[36–38] and ether-based[39] electrolytes, which is mainly attributed to the formation of a robust inorganic NaF-contaning/-rich SEI that inhibits Na dendrites and enabled homogeneous Na deposition, and thus improves cycling performance. Besides, there was reported that lower gas evolution and no degradation of EC and DMC was monitored in 1 M $NaPF_6$-EC:DMC (1 : 1 w/w) electrolyte against Na metal when 3 wt.-% FEC is used.[36] Also, an effective inhibition of self-discharging of Na//Hard Carbon cells was observed in the electrolyte 1 M $NaPF_6$-EC:DEC (1 : 1) when 10 % FEC had been added, but at the cost of increased polarization voltage.[16] However, there are also contradictorily negative effects of FEC on Na metal in certain concentrated electrolyte,[40] which could be attributed to the formation of a resistive layer composed of NaF that favors overpotential effects during Na plating/stripping.

Besides, the above-mentioned oxalate-salt NaDFOB, which were used as the electrolyte salt in few studies for carbon-based or Na-metal anodes, has demonstrated an effective improvement in terms of ionic conductivity, rate capability and cycling performance.[24,27] The use of NaDFOB was mainly inspired by the positive characteristics of its lithium analogue LiDFOB, namely the improvement of the SEI layer,[6,41–43] the reduction of transition metal solubility from the cathode[43–45] and the related prevention of shuttle transport of transition metal ions to the anode. Especially for Na metal anodes, the SEI formation involved NaDFOB was composed of robust inorganic borate-rich layers, which could preventing the decomposition of organic solvents,[25] optimize Na dendrite growth and suppress degradation of the SEI.[26] Also, NaDFOB anions has showed the ability to form a stable cathode electrolyte interphase (CEI), when it was used as conducting salt likely polymerized to form favorable CEI on FeF_3-carbon cathode,[28] with NaTFSI together formed $Na_xBO_yF_z$ species on NVP cathode,[27] as one of additives enhanced CEI layer on polyanionic NVPF ($Na_3V_2(PO_4)2F_3$) cathode,[46] or as a source of the conducting salt itself.[47] Additionally it was shown that NaDFOB is able to suppress Al corrosion in SIB.[48] However, as NaDFOB has not yet attracted much attention and little is known about the interaction between the conducting salt and the NaDFOB additive, there is a need for further research.

In order to understand the effects caused by these two additives, we employed them for stabilizing the cyclability of Na metal batteries; the additive FEC and NaDFOB was used at low concentration (1-2 wt-%), individually or combinedly, in the baseline electrolyte 1 M $NaPF_6$ – EC:PC (1 : 1 mol.%) and herein we tried to compare their positive contributions and detrimental effects on the chemical stability, sodium deposition of Na metal anode, and on the cycling stability of SMBs with Na anode and carbon-coated $Na_3V_2(PO_4)_3$ cathode. Firstly, we investigated how the reductive behaviors and oxidative stability were changed when additives were added, which was correlated to the formation and stability of the interface layers on both electrodes. For Na-plating/results, our study offers strategies by additive engineering.

Materials and Methods

Ethylene carbonate (EC, Huntsman, ultrapure) was used as received. Propylene carbonate (PC, ACROS, anhydrous 99.7 %) and pentane (Sigma Aldrich, anhydrous, $\geq$ 99 %) were dried with 3 Å molecular sieve and clarified by filtration. Sodium hexafluorophosphate ($NaPF_6$, Alfa Aesar, > 99 %) and sodium difluoro(oxalato) borate (NaDFOB, boron molecular, $\geq$ 95 %) were dried under vacuum at 105 °C for 2–3 days. Platinum plates, copper foil (Nippon Foil Mfg. C., Tokyo, Japan), Aluminum foils (Hohsen Corp. Japan, current collector quality, firstly cleaned with isopropanol), glass microfiber separator (Whatman®, GF/B with 0.68 mm thickness) and the calandered electrodes based on hard carbon (HC, active mass of ca. 300 mAh g^{-1}, coated on Al current collector, area-specific capacity

ca. 0.783 mAh cm^{-2}) and carbon-coated $Na_3V_2(PO_4)_3$/C (NVP or NVP/C, active mass of ca. 104 mAh g^{-1}, coated on Al current collector, area-specific capacity of 1 mAh cm^{-2}, synthesis process referred to[49]) were dried at 110 °C under vacuum for 2–3 days. Sodium electrode slices were prepared from sodium cubes (Sigma Aldrich, contains mineral oil, 99.9% trace metals basis). The most of mineral oil on a sodium cube was firstly removed by filter paper. Subsequently, the surface oxidation layer of the cubes was removed with stainless steel (SS) knife and the fresh sodium cubes were divided into slices with possibly similar thickness. The fresh piece was putted between two non-stick plates of Teflon or SS and this "sandwich"-type structure was pressed by using a hydraulic presser or a roller, until the slice was pressed into a desirable size (about 0.6 mm–0.8 mm). The pressed slices were dipped into the pentane and dried in the glovebox in order to remove any of the remaining mineral oil. The preparation of the electrolytes and sodium foils was conducted in an argon-filled glove box (MBraun GmbH) with oxygen and water levels below 0.5 ppm.

Electrolyte preparation. The electrolyte 1 M $NaPF_6$ is mixed in 1 : 1 mol.% EC:PC as baseline electrolyte mixture. Additionally, two kinds of additives, namely NaDFOB and FEC, are used in order to improve the baseline electrolyte. In case of NaDFOB, the main conducting salt $NaPF_6$ was reduced to keep the 1 M concentration constant; therefore, 0.1 M and 0.2 M NaDFOB were added accordingly. In this case, 0.1 M NaDFOB equals to 1.2 wt.% of the whole electrolyte weight. As simply marked in the following text and graphs, we use "1% NaDFOB". Secondly, FEC is used to replace 1 mol.% of all solvents, which equals ca. 2.2 wt.% of the whole electrolyte weight. We use "2% FEC" in the following graphs and text.

The **ionic conductivity** of the electrolytes was measured by the standard complex impedance method, with a Zahner Zennium IM6 electrochemical workstation in the frequency range from 1 kHz to 1 MHz, as described previously in detail[10] and in the supporting information in brief.

Cyclovoltammograms (CV measurement) or linear sweep voltammetry (LSV) were measured with a Zahner XPOT potentiostat (software: PPSeries, Potentiostat XPot Zahnerelektrik 6.4). The potential range of an anodic scan was set to 2.3–6.5 V vs. Na/Na^+ (below as V_{Na}) with platinum (Pt) as the working electrode. The reduction scan was conducted between 2.5 V vs. Na/Na^+ and 0 V vs. Na/Na^+ with copper (Cu) foil as the working electrode. The cells were measured in two-electrode configuration (EL-Cells manufactured by EL-Cell GmbH) with sodium metal reference electrode. The scan speed applied for all CV tests was set to 1 mV s^{-1}. To perform the Na-plating test, after 80 full cycles between 0.1–0 V vs. Na/Na^+, the scan potential was applied to −1 V vs. Na/Na^+ to conduct the sodium deposition on the copper foils. For a long-term cycling, the impedance measurements were performed on the cells before cycling, after 2, 10, 50 cycles and after every 100 full cycles.

The **chemical reactivity** of the electrolytes against Na was studied in two-electrode Swagelok®-cells with aluminum foils and sodium electrodes to track the open-circuit voltage changing with time.

For the **Na-plating/stripping** test in Na||Na symmetrical cells, these cells were firstly cycled at selected current densities (0.05 mA cm^{-2} to 4 mA cm^{-2}) for a certain time, and for every current density, the cycling was repeated 4 times. After high current density cycling, the cells were cycled again at lower current (0.5 and 1 mA cm^{-2}). A longer Na-plating/stripping cycling was done in those symmetric cells, which were cycled at 0.5 mA cm^{-2} for 1 h (until 0.5 mAh cm^{-2}) for every cycle, and thereafter, the impedance tests were performed.

The **Na metal half cells** (Na||NVP) were assembled in CR 2032 coin cell configuration (PI-KEM, Tamworth, U.K) with a digital, pressure-controlled electric crimper (MSK-160E, MTI corporation) at approximately 0.8 T in an argon-filled glove box according to standard procedures. The **full cells** (HC||NVP) were built from Hohsen cells (size: 2032). In detail, a hard carbon anode (HC, Ø = 16 mm), a NVP cathode (Ø = 16 cm), and a glass fiber separator (Whatman, GF/B: Ø = 17 mm with 160 µL electrolyte in case of half cells or QMA: Ø = 17 mm with 110 µL electrolyte for the full cells) were used inside the coin cell with one spring and one stainless steel spacer. The cycle stability of the Na||NVP cells was evaluated by galvanostatic cycling measurements between 2.3–3.8 V vs. Na/Na^+ at room temperature (25 ± 1 °C), and the cell cycling started at 0.1–0.5 mA cm^{-2}, and then continued at 0.5 mA cm^{-2} (charging, desodiation from NVP cathode) and 1 mA cm^{-2} (discharging, sodiation into NVP) until the cell fails. The HC||NVP full using Basytec cell cycler) and were cycled between 2.3–3.9 V vs. Na/Na^+, starting at 0.1 C for 2 cycles respectively, and then continued at mentioned in the. The materials for full cell are described in detail in reference.[50]

Three electrode cells from EL-Cell GmbH were assembled in an Ar filled glove box with a NVP foil (Ø = 16 cm) as cathode/working electrode (WE), a Na foil (Ø = 15 cm) as anode/counter electrode (CE), and a stacking of aluminum foils (Ø = 1 cm) as reference electrode (RE) between two glass fiber separator (Whatman, GF/B; Ø = 17 mm, with 320 µL electrolyte). Due to the chemical reactivity of sodium metal with carbonate electrolyte, aluminum was selected as reference material. Before the galvanostatic cycling, the three electrode cells were kept for three minutes in open-circuit status, so that the stable potential difference between Na and Al electrode was used to calibrate the initial potential of Al reference electrode. Based on this calibration potential value and measured potential difference (between WE and RE, and between CE and RE), the "real" potential of WE (vs. Na/Na^+) and of CE (vs. Na/Na^+) was obtained.

Results and Discussion

Electrolytes and Additives

The electrolytes employed in this work are based on the salt $NaPF_6$ (1 M, or 1 mol/L), which is dissolved in a mixture of two cyclic carbonates, namely EC and PC. Such a combination of carbonates has already been described in literature before and proofed to be a stable and suitable electrolyte mixture for the study.[10,19,46,50] In order to investigate the electrochemical interface formation and to enhance the cell operating efficiency, two promising additives, namely FEC and NaDFOB were used in different ratios, as shown in Table 1. One sample including both additives was also included to evaluate the synergistic effects.

One of the most important characteristics of the electrolyte is its ionic conductivity, which is shown in Figure 1. The 1 M $NaPF_6$ based electrolyte formulations exhibit ionic conductivity values in the order of 7.0 ± 0.4 mS cm^{-1} at T = 25 °C. The use of additives has no significant effect on the ionic conductivity of the electrolyte, either at room temperature or for the temperature-dependent values between 15 °C and 55 °C. It can be seen that the temperature-dependent conductivity values increase by a factor of ~2.4 when the temperature in increase by 40 °C. There was only a slight decrease in ionic conductivity with increasing NaDFOB content, while the use of FEC did not change the value. This is related to the fact that ionic NaDFOB

Table 1. The composition of the baseline electrolyte and electrolyte mixtures with additive used in this work.

sample	salt	solvent	additive
Baseline	1 M $NaPF_6$	EC + PC	–
"1 % NaDFOB"[a]	0.9 M $NaPF_6$	EC + PC	NaDFOB, 0.1 M
"2 % NaDFOB"[a]	0.8 M $NaPF_6$	EC + PC	NaDFOB, 0.2 M
"2 % FEC"[a]	1 M $NaPF_6$	EC + PC	FEC, 2 wt.%
"1 % NaDFOB + 2 % FEC"[a]	0.9 M $NaPF_6$	EC + PC	NaDFOB, 0.1 M, FEC, 2 wt.%

[a] The note of percentage is refered to the whole electrolyte weight (To note the electrolyte simply, the real percentage of additive is simplified: "1 % NaDFOB" = 1.2 wt.%, "2 % NaDFOB" = 2.4 wt.%, "2 % FEC" = 2.2 wt.% of the whole electrolyte or 2.26 mol-% of the all solvents).

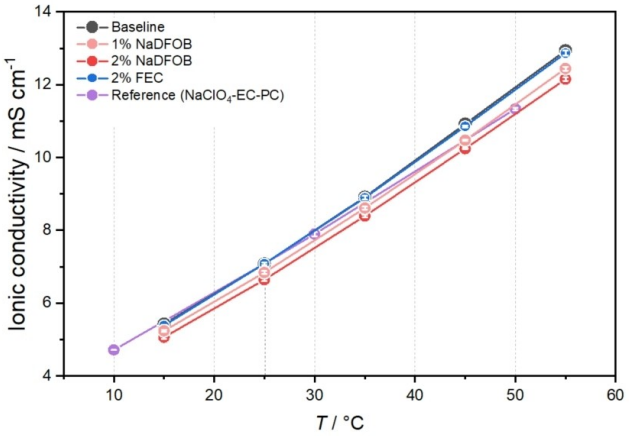

Figure 1. The ionic conductivity (mS cm^{-1}) of baseline and selected electrolyte mixtures with/without FEC or NaDFOB.

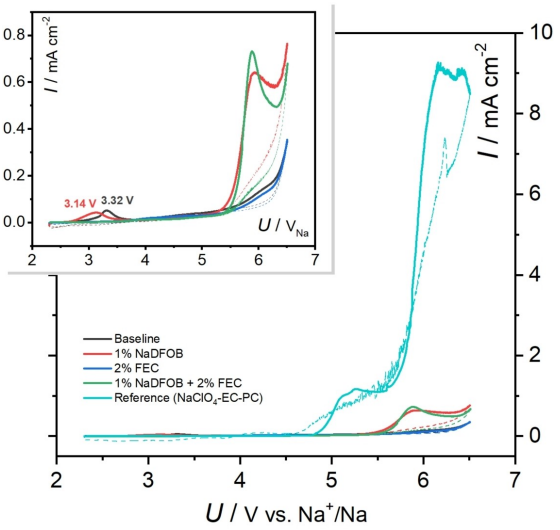

Figure 2. The oxidation stability of the selected electrolytes by Cyclovoltammetry measurements between 2.3 V_{Na} and 6.5 V_{Na} for Na||Pt cells.

salt affects the solvation of Na^+ ions and consequently increases the intermolecular interactions.[27,29] In addition to the $NaPF_6$-containing electrolytes, an electrolyte containing $NaClO_4$ with an identical electrolyte solvent composition was studied for its conductivity (6.6 ± 0.3 mS cm^{-1} at $T = 25$ °C). It should be noted that in the case of sodium conducting salts, very similar conductivity values are obtained regardless of the conducting salt anion.

Oxidation Stability and Cathodic Characteristics

The electrochemical stability of electrolyte and its electrochemical behavior at the interfaces are important criteria for the selection of suitable electrolytes. Firstly, the stability of the electrolyte in terms of electrochemical oxidation in a sodium cell scenario, for example at the high potential applied on the cathode side, was investigated in Na//Pt cells. Pt was used in the study to exclude intercalation/insertion of cathode material and to be consistent with references. As shown in Figure 2, the electrolyte reveals a stable oxidation resistance voltage up to 5.3 V vs. Na/Na^+ (in the following mentioned as "V_{Na}") with or without additives, and this stability seems to be determined by the baseline electrolyte components. The use of NaDFOB (red and green samples) leads to a large oxidation peak at $E = 5.5$–6 V_{Na}, i.e. related to the possible $DFOB^-$ anion reaction. However, this voltage is outside the range of potentials usually required for sodium cathode materials. As can be observed from the inset view, the baseline electrolyte shows a small oxidation peak at $E = 3.3$ V_{Na}, while the NaDFOB-electrolyte shows a peak at a lower potential ($E = 3.1$ V_{Na}), which might be related to the oxidation reaction of NaDFOB. The formation of the cathode electrode interface (CEI) through oxidation of NaDFOB and its influence on the cell cycling will be discussed below. The oxidation reaction peak between $E = 3.1$–3.3 V_{Na} is absent in the electrolyte sample that contain FEC. Consequently, the absence of the peak in the FEC/NaDFOB electrolyte could indicate the oxidation of FEC at lower potentials ($E < 3$ V_{Na}), which causes further oxidation reactions to be suppressed. Additionally, FEC can directly influence the molecular structure (e.g. solvation, SEI) of the salt-solvent system in order to have an impact on the oxidative stability of the electrolyte and interface layer.[51,52] Such an effect can influence the oxidation kinetics of NaDFOB, resulting in the observation of a small peak or not.

The reference electrolyte with $NaClO_4$ as conducting salt[10] showed a slightly lower oxidative stability, i.e. the new oxidation peak started from 4.75 V_{Na}, and followed by a larger peak, which is attributed to the oxidation reaction of the perchlorate ion.[53] Besides the anodic stability, a cathodic scan of the electrolyte ($E = 2.5$–0 V_{Na}) was carried out in order to elucidate interface reactions at cathode side (see Figure SI-1, supporting information). This clearly shows that different salts cannot simply be used in a complementary manner, even if individual measurements (e.g. conductivity) reveal almost no discrepancies.

As can be seen, when the Cu foil working electrode scanned cathodically towards $E < 0$ V_{Na}, a series of reduction peaks in early stage (i.e. in more positive potentials) were observed mainly in two areas, namely peaks between $E = 1.25$–1 V_{Na} and a

cascade drop below $E<0.75$ V_{Na}. It should be noted that the NaDFOB-containing electrolytes (green and red) have showed a gentle but broad peaks round $E=2$ V_{Na}, which indicated the reductive peaks in this more positive potential range, very likely related to the reduction reaction of NaDFOB.

To gain further insight into the dielectric properties of the interface layer and its passivation ability, Na plating experiment were performed on the SEI pre-formed Cu electrode (Figure 3). The electrolytes illustrated in Figure 3 have been firstly scanned on Cu working electrode of the Cu//Na cells for 80 cycles (between 0.1 and 0 V_{Na}), to facilitate the reduction chemistry on Cu and thus the interfacial layer formation, and after that, the electrochemical Na deposition was performed on the surface of this Cu electrode (by cathodic scanning to $E=-1$ V_{Na}). As can

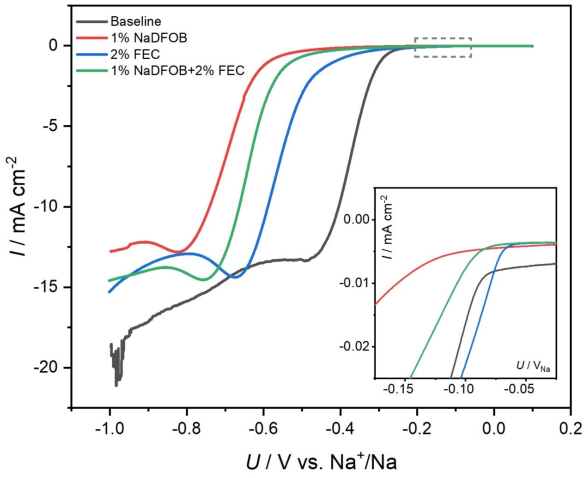

Figure 3. The Na metal plating on Cu foil of Na||Cu cells with different electrolyte mixtures triggered by a cathodic scan from 0.1 to -1 V_{Na}, directly after 80 cycles of Cu working electrode being polarized between 0.1 and 0 V_{Na}.

be seen from the figure, a successful Na deposition was observed below the negative direction of $E=-0.075$ V_{Na} and $E=-0.125$ V_{Na} (inset). However, the electrolytes exhibit a different plating manner in terms of on-set voltage and deposition rate. Overall, the behavior with both additives (green line in Figure 3) is between the two samples with the individual additives, suggesting that the SEI film formation and its effect on Na deposition can be generally adjusted through the ratio of both additives.

We have summarized some available experimental results and theoretical calculations of the reduction potentials of the relevant components in the literature on sodium (and lithium) batteries (Figure 4). The observed broad plateau of NaDFOB-electrolyte at around 2 V_{Na} is in line with literature reports,[25,28] indicating that NaDFOB could be preferentially reduced prior other solvent. This allows the early formation of a more robust inorganic-involved solid electrolyte interphase (SEI).[54] It can be seen that the reduction reaction between 1.25–1 V_{Na} can mainly be attributed to EC. In contrast, the subsequent onset of the cascade reduction current is due to a mixture of reduction reactions, including $NaPF_6$, PC and possibly FEC.

The inorganic additive NaDFOB appears to make the formed SEI film more resistive, due to the fact that the sample needs to be scanned to a negative voltage to obtain the same plating current density, which could be related to the more inorganic boron-containing components formed in the interface layer.[6,41–43] In contrast, FEC appears to result in an interface layer formation that is more receptive to electron transfer and lower dielectric properties, and therefore easily trigger the reduction of Na ions and deposit nucleation of Na. This suggests that it is possible to adjust the properties of interfaces by using both additives.

In addition, a long-term cycling of a cathodic scan between $E=0.1$ and $E=0$ V_{Na} was also conducted in Cu//Na cell in order

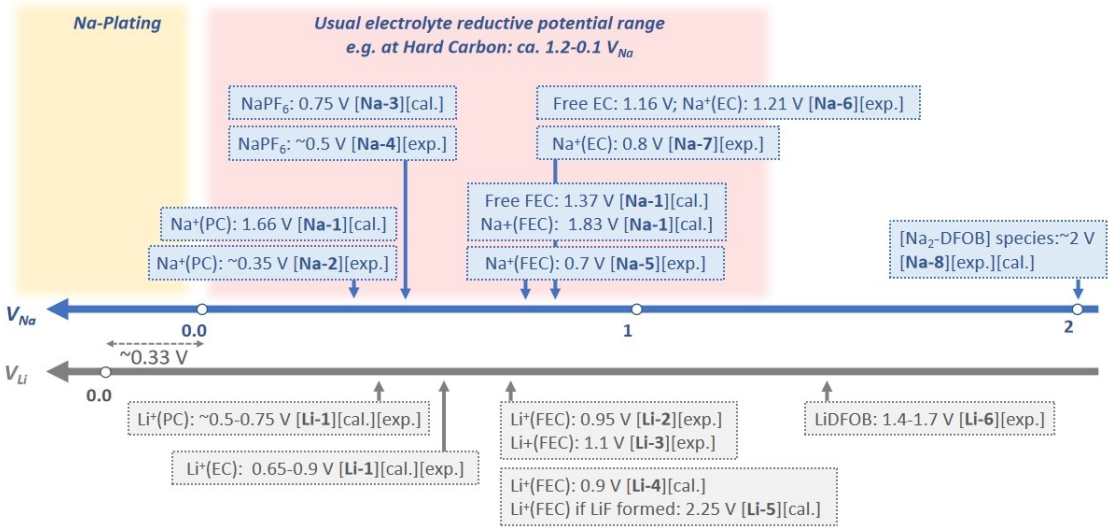

Figure 4. A schematic overview of the reduction potentials (vs. Na reference electrode, as V_{Na}) of the involved solvent, salt and additive molecules in Na environment by reviewing the published papers. For comparison, the reduction potentials (vs. Li, as V_{Li}) of the solvent molecules, FEC and LiDFOB in Li environment is also depicted. The annotates of [exp.] and [cal.] indicate the given values obtained by experiments and theoretical calculation. The potential values noted by [Na-1] to [Na-8] are referred to [55], [56,57], [58], [59], [60], [61], [62], [25,28] and the values by [Li-1] to [Li-6] to [63], [64], [65], [35,51,66], [35,66], [35,41,67,68], respectively.

to form the interface layer on the Cu working electrode. During the long-term cycling over 3,000 cycles, the impedance was measured after every certain cycle (see Figure SI-2, supporting information). The results show that the impedance varies with cycles, which indicates that the different additives strongly influence the formation of the interface. For the baseline sample, the impedance increases continuously with the cycle time and it takes about 1,400 cycles until a stable impedance is achieved, i.e. a stable interface is formed, whereas cells using the additives achieve stable impedance behavior within only 10–100 cycles.

Plating and Stripping of Sodium Metal

Reversible and stable sodium metal deposition as well as Na stripping is a crucial requirement for a practical application of sodium metal anodes. On the one hand, a highly efficient deposition process is important in reducing irreversible charge carrier losses; on the other hand, the irreversibly deposited sodium can induce dendrite growth and continuous electrolyte depletion, resulting from the electrochemical contact between the sodium metal and the electrolyte.[1,2,4,69] This process strongly depends on the interfacial layer and its stability, especially with respect to fast charge and discharge rates, as well as at low temperatures.The study of the overpotential of a symmetrical Na||Na cell cycled at selected current densities is shown in Figure 5. The resulting polarization potential of the Na plating/stripping cycle shows a clear dependence on the cycling rate, which can be attributed to the limiting factors of ion conduction and interfacial reaction kinetics within the symmetric cell. The overall trend, i.e. the polarization potential, increases gradually with increasing cycle currents. For example, it remains low, i.e. from as low as $I = 0.1–0.15\ mA\,cm^{-2}$ for baseline electrolyte up to $j = 0.2–0.25\ mA\,cm^{-2}$ for NaDFOB, when current density is applied to the cell at $j = 0.05–0.5\ mA\,cm^{-2}$. At higher current density values ($j = 1–4\ mA\,cm^{-2}$), the increase in current is not proportional to the increase in polarized over-potential, i.e. the overpotential increases more rapidly. For example, for NaDFOB, the potential increases from 200 mV to 250 mV for a current density increase from $0.05\ mA\,cm^{-2}$ to $0.5\ mA\,cm^{-2}$ (10 times), but from 300 mV to 400 mV for a current increase from $1\ mA\,cm^{-2}$ to $2\ mA\,cm^{-2}$ (2 times), at which point the ion diffusion behavior in the electrolyte seems to become the limiting factor (see Figure 1). This could also be directly related to the rate-capability of the sodium-metal anode cell, as shown below.

For the different additives, it can be concluded that the additive-free and FEC samples show a relatively lower over-potential, regardless of the rate at which they are cycled, while the potential of NaDFOB based electrolytes is relatively high, which correlates with the higher electric resistance of the formed interfacial layer at Na electrode side, a fact that is supported by the more negative plating voltage in the previous Na//Cu cell (Figure 4). Overall, the results for the samples with

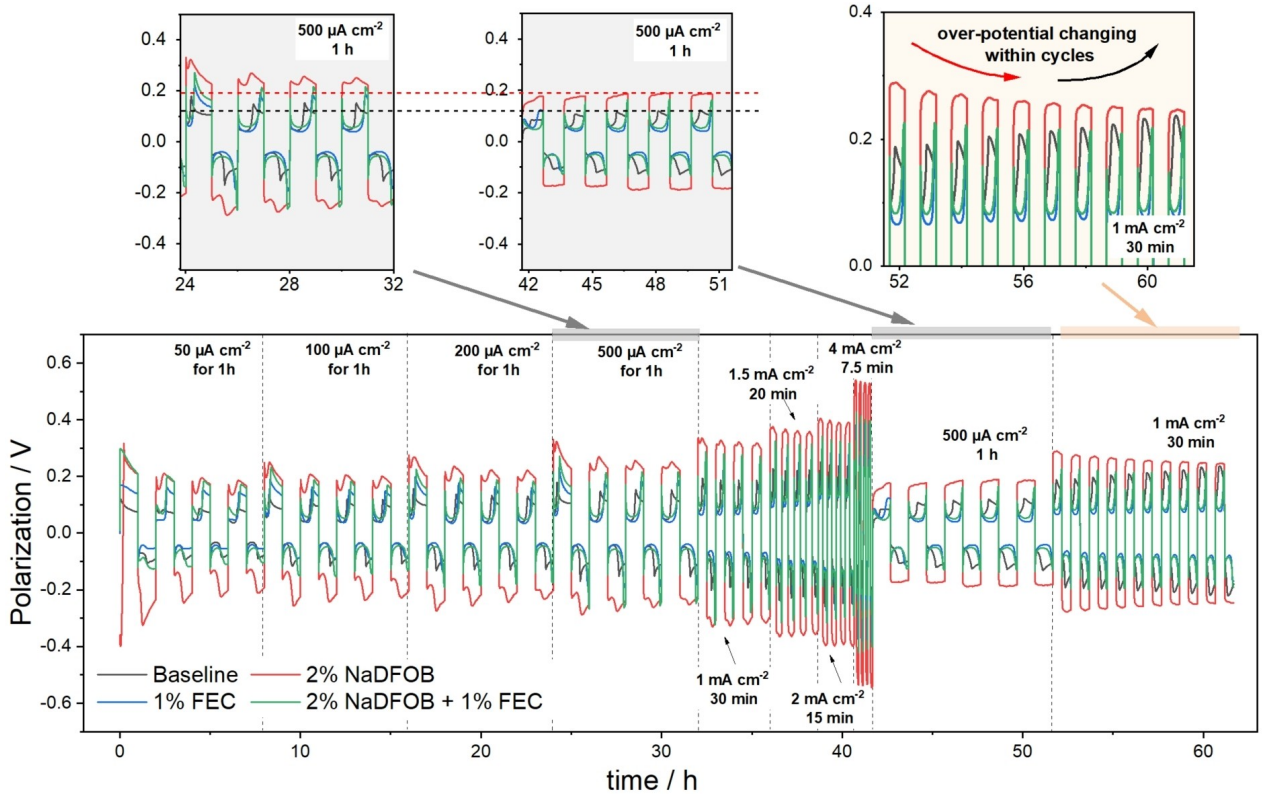

Figure 5. The Na plating/stripping cycling at various current densities in a Na||Na-symmetric cell with the electrolyte mixtures. The current densities and the duration for each half cycle was marked on graph.

both additives were essentially between the results with one additive alone.

Several aspects are also worth mentioning. First, after cycling at a higher current rates (between 1 and 4 mA cm^{-2}), the symmetric cells show a clear overvoltage drop and stabilization (independent of the additives) as soon as they return to the lower deposition rate (e.g. 0.5 mA cm^{-2}) (see enlarged grey view at the top of Figure 5). An additional feature is observed with NaDFOB: After Na deposition at a high current rate, the plot appears "smoother", i.e. the potential peak that occurred before becomes flatter. This type of peak is related to the charge barrier caused by the interface, more precisely to the properties of the interface such as morphology, thickness, etc.[70] The disappearance of the peak can therefore be attributed to the fact that the high speed of the deposition/dissolution process led to a reconfiguration of the interface with NaDFOB, resulting in a more homogeneous (in terms of electrical potential) Na deposition/dissolution. In addition, the results of the subsequent long-term cycles (Figure 5, below) confirm that this "smoothing effect" occurs not only at high current rate, but also after a higher number of cycles.

It is also remarkable when looking at the cells cycled at a current rate of $j = 1$ mA cm^{-2} between $t = 51.5$–61.5 h (enlarged inset in the top right of Figure 5) that the overvoltage profile shows an opposite trend during cycling: the overvoltage of the electrolyte without additives slowly increases significantly, while the overvoltage decreases and becomes almost stable in the case of the additive NaDFOB, and remains almost unchanged in the case of FEC. In contrast, the overpotential of the base electrolyte was not significantly destabilized in the previous cycles at the corresponding current rate of $j = 1$ mA cm^{-2} (at $t =$ 32–36 h), which is probably related to its greater sensitivity to the higher current rate respectively to the plating/stripping; in contrast, NaDFOB showed a dynamic stabilizing effect on the Na-metal interface. These properties need to be comparatively investigated by long deposition cycles (see supporting information, section 3, Figure SI-3, including remarks) which reveal that the usage of FEC indeed tune the interface layer properties, affecting the Na deposition.

The EIS results obviously suggest that the magnitude and changes in interfacial impedance are highly correlated with the plating-stripping stability, and that the additives has a positive role in modulating the interface and therefore influencing metal deposition. The same characteristic can be seen even more clearly at higher current rates ($j = 1$ mA cm^{-2}, see Figure SI-4, supporting information), which also confirm that only the electrolyte sample mixed with both additives exhibits almost stable response over a time period of $t = 300$ h, i.e. a stable overvoltage of approximately $E = 0.5$ V_{Na}.

Chemical vs. Electrochemical Na-Passivation

For active lithium and sodium electrodes, the mostly engaged electrolytes are not strictly chemically inert, but the chemical passivation on the alkali metal surface (which can also be considered as pre-formed interface) and the effectiveness of this passivation process in preventing further side reactions are essential for stable battery cycling. A possibility to clarify the chemical or electrochemical reactivity is to carry out open-circuit voltage (OCV) measurements.

The results (see supporting information, Figure SI-5) illustrate the change in Na electrode potential (difference) in the open circuit state because of the interfacial chemistry reaction of Na with electrolyte in a newly assembled Na||Al cell. Additionally, EIS measurements are recorded to compare the characteristics of the interfacial layer. Based on the measurement it can be concluded that the interfacial reaction at the sodium-metal electrode exhibits three main stages, namely an initial very short period of interfacial passivation with a rapid rise in voltage, followed by a maximum (a period of stabilization), and voltage plateau. After a relatively stable period of approx. 500 h, changes can be seen in the different mixtures. For example, the potential difference decreases sharply again in the case of the base electrolyte, whereas it increases with the pure NaDFOB electrolyte and remains almost constant with the FEC-mixed electrolytes. Although the interfacial chemistry cannot be identified exactly, these results are closely related to the destruction of the interfacial layer (such as by dissolution), or possibly the occurrence of a new reaction to create a more stable interface layer. EIS measurements (Figure SI-5) reveal that the baseline electrolyte produces a higher resistance interfacial layer due to the breakdown of the primary interface and consequently side reactions, while the resistance of the interface formed in NaDFOB electrolyte can be attributed to the thickening of the interface. Two impedance semicircles of differing size can be observed in FEC samples, indicating that the interface involved in FEC exhibits less dense surface films (smaller first semicircle, i.e. the SEI resistance). However, given the ionic conductive nature of the interfacial layer, electrolyte with both additives shows lower resistance (bigger second semicircle of FEC, i.e. charge transfer resistance), beneficial for ion diffuse through interface layer. After disabling the coin cells (Figure SI-5) the surface of the sodium metal remains almost clear for FEC based electrolyte and slightly grayish for the other electrolytes. Additionally, the yellowish separator in case of baseline electrolyte confirms that passivation without additives is not consistently effective in preventing electrolyte side reactions.

The effectiveness of the electrochemically passivated interface on the electrode in preventing electrolyte side reactions is compared in Figure 6a which shows the cycling stability results of the cellsthat have undergone electrochemical charging and discharging after a different "rest" (open-circuit condition) periods. It is obvious that the baseline electrolyte already exhibits a drop in the cell discharge capacity before the first break, and subsequently after 7 months of pausing, only a small amount of capacity was regained indicating a rapid battery failure. This is likely to be related to the damage to the interface that had been built up before cell rest, and hence the loss of passivation ability and consequently electrolyte side reactions.

In contrast, NaDFOB and FEC containing cells still operate quite stable after the first break. After another 2 months of cell rest storage, both electrolytes still performed excellently, except

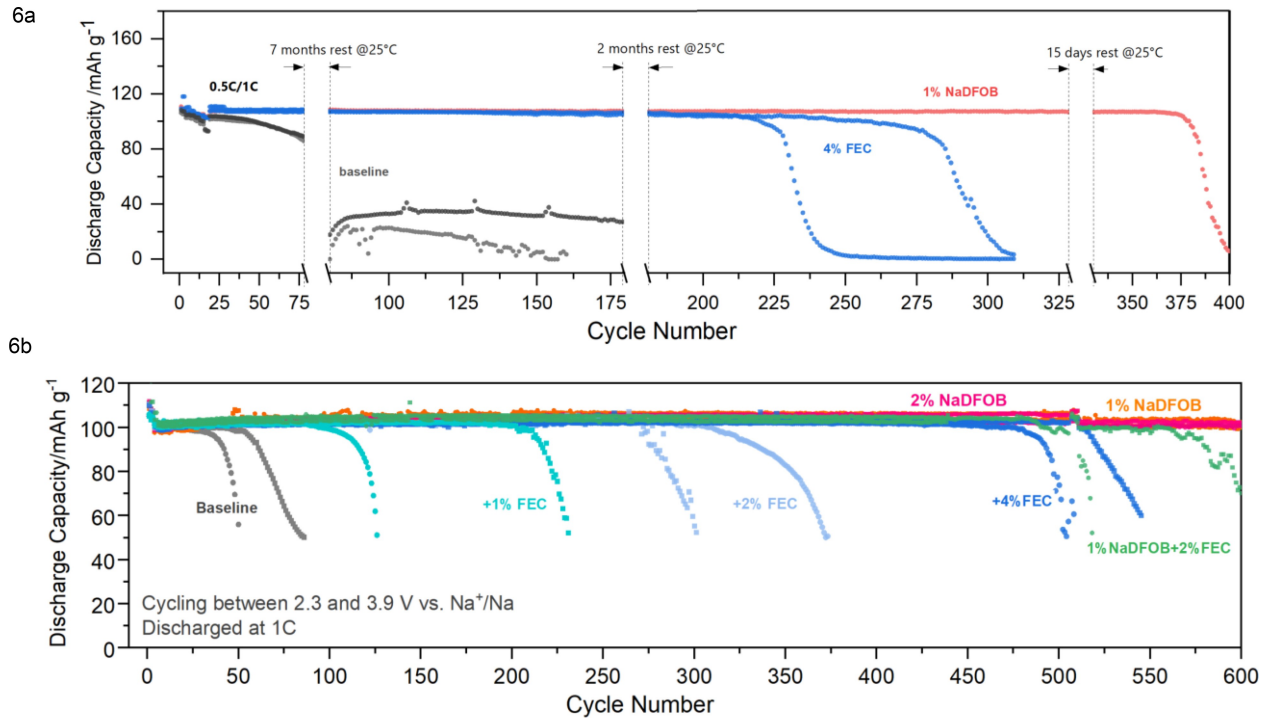

Figure 6. a) The discharging capacity in the galvanostatic cell cycling of the sodium anode cells (Na||NVP) with 3 times cell "rest" where the cell cycling being stopped at the end of discharging to 2.3 V and then being storaged at 25 °C under insulated conditions for different duration (Exceptionally, the 15-day rest is due to a technical fault on cycler). 6b) The discharging capacity (discharging: 1 C and charging: 0.5 C) in the galvanostatic cell cycling (2.3 and 3.9 V) of the sodium anode cells (Na||NVP) with electrolyte mixtures. The interupt of the cell cycling at 520st. cycle is due to the technical error (power breakdown), and after short shutdown, the cells were renewly cycled.

that FEC gradually lost its capability. NaDFOB, in contrast, again experienced a short battery rest before battery failure occurred. This indicates that FEC and NaDFOB (superior) as electrolyte additives clearly improve the effectiveness of the electrochemical interface on the susceptible Na anode for passivation in the electrolyte and can maintain the capacity even after long periods of open circuit storage.

Cell Cycling and Cell Performance in Half Cell Tests Against Sodium Metal

In this chapter, the test results of coin cells with sodium metal anodes are presented. As can be seen from the cycle results of Na||NVP coin cells (Figure 6b), the use of additives significantly increased the cycle life of the cells compared to the baseline electrolyte. In particular, a 1–2% NaDFOB as additive resulted in stable cell cycling up to 600 cycles. For the FEC, the observed improvement in battery performance is highly dependent on the amount of additive used, and small amounts (1–2%) seem to make a limited positive contribution, meaning that the right amount can achieve very good results. Additionally, this supports the hypothesis that FEC is continuously consumed during cycling. The use of both additives also benefits the stability of the battery cycling.

It should be noted that the charge and discharge curves provided in Figure 6b show the potential difference between two electrodes and do not give a sufficient insight into the details of the electrochemical processes inside each electrode and its interface. For this purpose, the cycling of three-electrode cells can be used to understand both main electrochemical processes, namely the deposition and stripping of Na at the Na negative electrode ($E_{CE} = E_{(counter\ electrode)}$; see supporting information, Figure SI-6–SI-9) and the simultaneous insertion and removal of Na^+ ions from the NVP positive electrode ($E_{WE} = E_{(working\ electrode)}$; Figure 7). For the charge/discharge profiles of the cathode material NVP (E_{WE}), a voltage hysteresis is well observed, which can be related to differences in the kinetic factors of the Na^+ ions in the charge and discharge process. That means that the diffusion process of the sodium ions embedding in the NVP material during the discharge process is slower than the ionic removal during the charging process.[71]

As the same electrodes were always used in this work, this hysteresis can be related to the formed cathode interface layer (CEI) causing ion diffusion resistance and its effect on the kinetic differences during the charging/discharging processes. In other words, the interphasial energy barrier for ion transfer plays a critical role in the voltage hystersis, similar to which has been discussed in relation to the interfacial resistance through the SEI film at the graphite anode.[72] For the baseline electrolyte, the voltage hysteresis is minimal at the beginning of the cycling ($\Delta E = 18$ mV in the 5th cycle). However, the hysteresis voltage of the cells with baseline electrolyte increases significantly with cycling ($\Delta E = 231$ mV in the 50th cycle).

For the NaDFOB electrolyte, the voltage hysteresis is much higher at the beginning of the cycling (factor of 11 compared

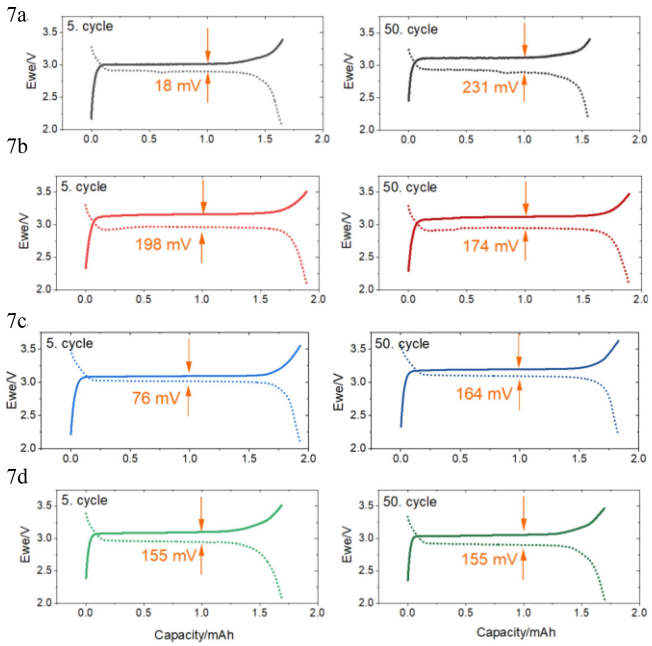

Figure 7. The charging-discharging potential profiles of the three-electrode cells with NVP as working electrode (WE), Na as counter electrode (CE) and Aluminum as reference electrode (CE) for the electroyte mixtures (7a: baseline, 7b–7d) electrolytes with NaDFOB, FEC and two additives, respectively). The potential profiles of the working electrode (E_{WE} vs. V_{Na}) showed here are selected at the 5th and 50th cycles at approximately 1.018 mA cm^{-2} (~1 C, referred to nominal discharge capacity of the 16 mm NVP/C cathode: 2.03 mA).

to the baseline electrolyte), which gives strong evidence for the formation of a resistant interfacial layer CEI that significantly hinders ion diffusion, which also corresponds to the new oxidation peak in the CV-measurements results (Figure 2). However, it is worth mentioning that this voltage hysteresis decreases with cycling corresponds to the results of the symmetric cell where also a decrease of the overpotential with cycling is observed. Although the FEC electrolyte has a smaller voltage hysteresis compared to the NaDFOB-containing electrolyte, indicating the less interfacial resistance, the hysteresis rises more significantly (50th cycle vs. 5th cycle). Such behavior revealed that the interface layer continuously changes under oxidative conditions and the cathode raises the barrier to ion diffusion, indicating that the interface formed by the FEC is less stable regarding to dielectric or electrochemically inertness. Interestingly, the NaDFOB electrolyte showed even decreased the voltage hysteresis (red) and unchanged value (green), which all revealed the interfacial stabilizing/stabilization at the cathode side.[28,46]

For the Na redox process (E_{CE} profiles, Figure SI-6,7,8,9) at the Na metal electrode, it can be seen that the use of the additives changes the potential profile of Na stripping. The NaDFOB containing electrolyte exhibits a higher stripping value (the more negative potential), which is associated with the formation of an interfacial layer with higher dielectric properties, and which is also consistent with the higher overpotential results in the symmetric cell tests (see Figure 5). The minor change in the stripping potential after a few tens of cycles is usually coupled with a small change on the discharge plateau in the $E_{WE\text{-}CE}$ curve (i.e. the actual charge/discharge operation curve of the Na anode cell, Figure SI-6,7,8,9).

Further, when comparing this cell result (Figure 6b, 7) with the symmetric cell (Figure 5), it can be seen that NaDFOB containing electrolyte exhibits not the best results, despite its improved reversible Na-plating/stripping cycling behavior, but showed a much better performance when the cathode material NVP was involved (instead of symmetrical cells). Thus, the interaction of NaDFOB respectively DFOB$^-$-anions with the cathode oxide materials plays a particularly important role in the cell cycling, as demonstrated by the voltage hysteresis results above.

Cell Cycling in HC||NVP Full-Cell Tests

The cycling capability of both additive electrolytes is investigated in coin cell configuration with hard-carbon (HC) negative electrode (Figure 8) as it is known that especially FEC worsen the cell performance in full cell configuration.[73] Different to the sodium metal anode cell, the baseline electrolyte (Figure 8a) exhibits a stable cell cycle capability when hard carbon electrodes are used (capacity retention of 98.5 % within 500 cycles, calculation based on the 0.1 C step at the beginning and at the end). The NaDFOB containing electrolyte also remained generally stable, although with a slightly lower capacity retention of 92.8 % (500 cycles, 0.1 C step as explained before).

The use of FEC, however, resulted in a more pronounced capacity fading within cycles (85.1 %, 500 cycles, 0.1 C step). In contrast, it seems to be contradictory that a more stable Na anode cell cycling could be enabled by FEC-electrolyte. The reason for the earlier capacity decline may be ascribed not (only) to NVP, but rather to the interaction of FEC with hard carbon anode, because FEC showed excellent effect on Na, and long-term cyclable Na//NVP cells, but faster capacity fading when HC anodes are used.

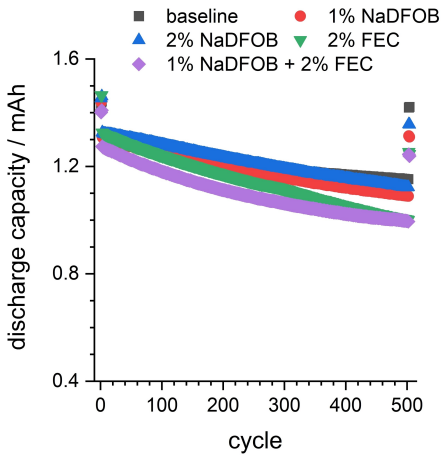

Figure 8. Long term cycling of HC||NVP cells at 1 C (CCCV, C/15) charge and 1.5 C discharge (CC only) with C/10 at beginning and end of cycling after 500 cycles.

According to the similar result reported before,[73] the increase of the overpotential between charge and discharge on HC against Na metal, due to SEI formation involved by FEC, might be a detrimental effect to the reversible capacity during cell cycling, since the full access of the low potential plateau at HC electrodes (ca. 0.1 V vs. V_{Na}) might be hindered. However, this effect of FEC on the electrochemical performance of cells is also strongly dependent of the salt used, owing to special contributions of different main components of SEI layer formed by using different salt, although the added FEC could enhance the formation of NaF in SEI.[74] In addition, the dQ/dV profiles (Figure SI-10, supporting information) of the low-rate charge/discharge curves reveal how the additives affect the intercalation platform of sodium ions at the electrodes and the electrolyte reactions in the full cell. It can be seen that after 10 cycles, the peaks at $E = 3.3$-3.4 V remain, attributed to the storage process of sodium ions in the positive and negative materials, while the additional peaks at $E = 2.3$ V and $E = 2.5$-2.7 V showed at first cycle, corresponding to the electrochemical interfacial reactions of the electrolyte.

These results demonstrate that the appropriate choice of additive for the electrode used plays a key role in tailoring the interface properties and resulting cell aging.

Conclusions

The study revealed that the two additives FEC and NaDFOB significantly improve Na-ion cell aging and the stabilization of the Na surface in Na half cells when used together with the carbonate-based electrolyte system EC + PC + 1 M $NaPF_6$. The cell storage tests, plating/stripping tests and impedance measurements indicated that the additives enable efficient formation of the interfacial layer. In particular, electrolytes containing NaDFOB exhibit a more positive reduction potential prior than other solvents, which benefits to form a robust SEI layer. At the same time, the symmetrical Na//Na cells show evidence of oxidative decomposition of the NaDFOB-containing electrolyte mixtures. The results of the full-cell tests also show that NaDFOB appears to be a very promising standard additive, as it does not impair the performance in the case of full cells (HC//NVP) like FEC, but at the same time significantly improves the half-cell tests. This is not the case with FEC, as the half cells are stabilized, but the full cells degrade significantly more strongly. It could be shown that even very small amounts of additives are highly effective and contribute to an improvement of the dynamic formation and stabilization processes at the interfaces. The tests of the three-electrode cell reliably indicated the significant changes in cathode potential during charging and discharging. It should be specifically pointed out that not only the sodium deposition process at the Na-metal anode but also the effect of additives on the electrochemical results of the cathode during cycling must be considered to improve the cycling performance of stable SIBs.

Acknowledgements

This work was funded by the Deutsche Forschungsgemeinschaft (DFG, German Research Foundation) under Germany's Excellence Strategy – EXC 2154 – Project number 390874152 (POLiS Cluster of Excellence), and contributes to the research performed at Center for Electrochemical Energy Storage Ulm Karlsruhe (CELEST). Open Access funding enabled and organized by Projekt DEAL.

Conflict of Interests

The authors declare no conflict of interest.

Data Availability Statement

The data that support the findings of this study are available in the supplementary material of this article. Additionally, raw data are provided at 10.5281/zenodo.14556036.

Keywords: Sodium ion battery · Additives · FEC · NaDFOB · Sodium Plating-Stripping

[1] Y. Zhao, K. R. Adair, X. Sun, *Energy Environ. Sci.* **2018**, *11*, 2673.
[2] D. Lin, Y. Liu, Y. Cui, *Nat. Nanotechnol.* **2017**, *12*, 194.
[3] Y. Lee, J. Lee, J. Lee, K. Kim, A. Cha, S. Kang, T. Wi, S. J. Kang, H.-W. Lee, N.-S. Choi, *ACS Appl. Mater. Interfaces* **2018**, *10*, 15270.
[4] C. Bao, B. Wang, P. Liu, H. Wu, Y. Zhou, D. Wang, H. Liu, S. Dou, *Adv. Funct. Mater.* **2020**, *30*, 2004891.
[5] J. Xu, J. Yang, Y. Qiu, Y. Jin, T. Wang, B. Sun, G. Wang, *Nano Res.* **2024**, *17*, 1288.
[6] K. Xu, *Chem. Rev.* **2014**, *114*, 11503.
[7] E. Peled, S. Menkin, *J. Electrochem. Soc.* **2017**, *164*, 1703.
[8] D. I. Iermakova, R. Dugas, M. R. Palacín, A. Ponrouch, *J. Electrochem. Soc.* **2015**, *162*, 7060.
[9] W. Liu, P. Liu, D. Mitlin, *Adv. Energy Mater.* **2020**, *10*, 2002297.
[10] A. Hofmann, Z. Wang, S. P. Bautista, M. Weil, F. Müller, R. Löwe, L. Schneider, I. U. Mohsin, T. Hanemann, *Electrochim. Acta* **2022**, *403*, 139670.
[11] D. Stottmeister, L. Wildersinn, J. Maibach, A. Hofmann, F. Jeschull, A. Gross, *ChemSusChem* **2024**, *17*, e202300995.
[12] Y.-S. Hong, N. Li, H. Chen, P. Wang, W.-L. Song, D. Fang, *Energy Storage Mater.* **2018**, *11*, 118.
[13] H. Liu, X.-B. Cheng, Z. Jin, R. Zhang, G. Wang, L.-Q. Chen, Q.-B. Liu, J.-Q. Huang, Q. Zhang, *EnergyChem* **2019**, *1*, 100003.
[14] Y. Deng, J. Zheng, A. Warren, J. Yin, S. Choudhury, P. Biswal, D. Zhang, L. A. Archer, *Adv. Energy Mater.* **2019**, *9*, 1901651.
[15] A. Le Ma, A. J. Naylor, L. Nyholm, R. Younesi, *Angew. Chem. Int. Ed.* **2021**, *60*, 4855.
[16] R. Mogensen, D. Brandell, R. Younesi, *ACS Energy Lett.* **2016**, *1*, 1173.
[17] M. Gauthier, T. J. Carney, A. Grimaud, L. Giordano, N. Pour, H.-H. Chang, D. P. Fenning, S. F. Lux, O. Paschos, C. Bauer, F. Maglia, S. Lupart, P. Lamp, Y. Shao-Horn, *J. Phys. Chem. Lett.* **2015**, *6*, 4653.
[18] J. Xu, *Nano-Micro Lett.* **2022**, *14*, 166.
[19] G. G. Eshetu, G. A. Elia, M. Armand, M. Forsyth, S. Komaba, T. Rojo, S. Passerini, *Adv. Energy Mater.* **2020**, *10*, 2000093.
[20] Z. W. Seh, J. Sun, Y. Sun, Y. Cui, *ACS Cent. Sci.* **2015**, *1*, 449.
[21] S. Wang, Y. Chen, Y. Jie, S. Lang, J. Song, Z. Lei, S. Wang, X. Ren, D. Wang, X. Li, R. Cao, G. Zhang, S. Jiao, *Small Methods* **2020**, *4*, 1900856.
[22] L. Zhou, Z. Cao, J. Zhang, Q. Sun, Y. Wu, W. Wahyudi, J.-Y. Hwang, L. Wang, L. Cavallo, Y.-K. Sun, H. N. Alshareef, J. Ming, *Nano Lett.* **2020**, *20*, 3247.
[23] B. S. Parimalam, B. L. Lucht, *J. Electrochem. Soc.* **2018**, *165*, 251.

[24] J. Chen, Z. Huang, C. Wang, S. Porter, B. Wang, W. Lie, H. K. Liu, *Chem. Commun.* **2015**, *51*, 9809.
[25] Lina Gao, et al., *Sci. Adv.* **2022**, *8*, eabm4606. DOI:10.1126/sciadv.abm4606.
[26] L. Gao, J. Chen, Y. Liu, Y. Yamauchi, Z. Huang, X. Kong, *J. Mater. Chem. A* **2018**, *6*, 12012.
[27] H. M. Law, J. Yu, S. C. T. Kwok, G. Zhou, M. J. Robson, J. Wu, F. Ciucci, *Energy Storage Mater.* **2022**, *46*, 182.
[28] Z. Sun, W. Fu, M. Z. Liu, P. Lu, E. Zhao, A. Magasinski, M. Liu, S. Luo, J. McDaniel, G. Yushin, *J. Mater. Chem. A* **2020**, *8*, 4091.
[29] C. Ge, L. Wang, L. Xue, Z.-S. Wu, H. Li, Z. Gong, X.-D. Zhang, *J. Power Sources* **2014**, *248*, 77.
[30] J. Zheng, S. Chen, W. Zhao, J. Song, M. H. Engelhard, J.-G. Zhang, *ACS Energy Lett.* **2018**, *3*, 315.
[31] M. Goktas, C. Bolli, J. Buchheim, E. J. Berg, P. Novák, F. Bonilla, T. Rojo, S. Komaba, K. Kubota, P. Adelhelm, *ACS Appl. Mater. Interfaces* **2019**, *11*, 32844.
[32] Y. Yamada, J. Wang, S. Ko, E. Watanabe, A. Yamada, *Nat. Energy* **2019**, *4*, 269.
[33] D. T. Duncan, I. E. Gunathilaka, M. Forsyth, D. R. MacFarlane, M. Kar, *Electrochim. Acta* **2023**, *472*, 143398.
[34] X.-Q. Zhang, X.-B. Cheng, X. Chen, C. Yan, Q. Zhang, *Adv. Funct. Mater.* **2017**, *27*, 1605989.
[35] S. A. Delp, O. Borodin, M. Olguin, C. G. Eisner, J. L. Allen, T. R. Jow, *Electrochim. Acta* **2016**, *209*, 498.
[36] R. Dugas, A. Ponrouch, G. Gachot, R. David, M. R. Palacin, J. M. Tarascon, *J. Electrochem. Soc.* **2016**, *163*, 2333.
[37] R. Rodriguez, K. E. Loeffler, S. S. Nathan, J. K. Sheavly, A. Dolocan, A. Heller, C. B. Mullins, *ACS Energy Lett.* **2017**, *2*, 2051.
[38] Q. Wang, C. Zhao, X. Lv, Y. Lu, K. Lin, S. Zhang, F. Kang, Y.-S. Hu, B. Li, *J. Mater. Chem. A* **2019**, *7*, 24857.
[39] M. Han, C. Zhu, T. Ma, Z. Pan, Z. Tao, J. Chen, *Chem. Commun.* **2018**, *54*, 2381.
[40] J. Lee, Y. Lee, J. Lee, S.-M. Lee, J.-H. Choi, H. Kim, M.-S. Kwon, K. Kang, K. T. Lee, N.-S. Choi, *ACS Appl. Mater. Interfaces* **2017**, *9*, 3723.
[41] Z. Chen, J. Liu, K. Amine, *Electrochem. Solid-State Lett.* **2007**, *10*, 45.
[42] Q. Dong, F. Guo, Z. Cheng, Y. Mao, R. Huang, F. Li, H. Dong, Q. Zhang, W. Li, H. Chen, Z. Luo, Y. Shen, X. Wu, L. Chen, *ACS Appl. Energ. Mater.* **2020**, *3*, 695.
[43] Y. Zhu, Y. Li, M. Bettge, D. P. Abraham, *J. Electrochem. Soc.* **2012**, *159*, 2109.
[44] A. Hofmann, A. Höweling, N. Bohn, M. Müller, J. R. Binder, T. Hanemann, *ChemElectroChem* **2019**, *6*, 5255.
[45] I. A. Shkrob, Y. Zhu, T. W. Marin, D. P. Abraham, *J. Phys. Chem. C* **2013**, *117*, 23750.
[46] G. Yan, K. Reeves, D. Foix, Z. Li, C. Cometto, S. Mariyappan, M. Salanne, J. M. Tarascon, *Adv. Energy Mater.* **2019**, *9*, 1901431.
[47] X. Liu, J. Zhao, H. Dong, L. Zhang, H. Zhang, Y. Gao, X. Zhou, L. Zhang, L. Li, Y. Liu, S. Chou, W. Lai, C. Zhang, S. Chou, *Adv. Funct. Mater.* **2024**, *34*.
[48] L. Huang, Q. Qiu, M. Yang, H. Li, J. Zhu, W. Zhang, S. Wang, L. Xia, P. Müller-Buschbaum, *ACS Appl. Mater. Interfaces* **2024**, *16*, 46392.
[49] T. Akçay, M. Häringer, K. Pfeifer, J. Anhalt, J. R. Binder, S. Dsoke, D. Kramer, R. Mönig, *ACS Appl. Energ. Mater.* **2021**, *4*, 12688.
[50] P. Stüble, C. Müller, J. Klemens, P. Scharfer, W. Schabel, M. Häringer, J. R. Binder, A. Hofmann, A. Smith, *Batteries & Supercaps* **2024**, *7*, e202300375.
[51] T. Hou, G. Yang, N. N. Rajput, J. Self, S.-W. Park, J. Nanda, K. A. Persson, *Nano Energy* **2019**, *64*, 103881.
[52] A. Wang, S. Kadam, H. Li, et al., *npj Comput Mater* **2018**, *4*, 15. https://doi.org/10.1038/s41524-018-0064-0.
[53] A. Bhide, J. Hofmann, A. Katharina Dürr, J. Janek, P. Adelhelm, *Phys. Chem. Chem. Phys.* **2014**, *16*, 1987.
[54] M. Liu, E. Zhou, C. Wang, Y. Ye, X. Tong, Y. Xie, S. Zhou, R. Huang, X. Kong, H. Jin, H. Ji, *Small* **2023**, *19*, 2208282.
[55] U. Purushotham, N. Takenaka, M. Nagaoka, *RSC Adv.* **2016**, *6*, 65232.
[56] Q. Li, W. Zhang, J. Peng, W. Zhang, Z. Liang, J. Wu, J. Feng, H. Li, S. Huang, *ACS Nano* **2021**, *15*, 15104.
[57] K. Tang, L. Fu, R. J. White, L. Yu, M.-M. Titirici, M. Antonietti, J. Maier, *Adv. Energy Mater.* **2012**, *2*, 873.
[58] C. Wang, A. C. Thenuwara, J. Luo, P. P. Shetty, M. T. McDowell, H. Zhu, S. Posada-Pérez, H. Xiong, G. Hautier, W. Li, *Nat. Commun.* **2022**, *13*, 4934.
[59] K. Wang, Y. Jin, S. Sun, Y. Huang, J. Peng, J. Luo, Q. Zhang, Y. Qiu, C. Fang, J. Han, *ACS Omega* **2017**, *2*, 1687.
[60] S. Komaba, T. Ishikawa, N. Yabuuchi, W. Murata, A. Ito, Y. Ohsawa, *ACS Appl. Mater. Interfaces* **2011**, *3*, 4165.
[61] K. Westman, R. Dugas, P. Jankowski, W. Wieczorek, G. Gachot, M. Morcrette, E. Irisarri, A. Ponrouch, M. R. Palacín, J.-M. Tarascon, P. Johansson, *ACS Appl. Energ. Mater.* **2018**, *1*, 2671.
[62] P. Thomas, J. Ghanbaja, D. Billaud, *Electrochim. Acta* **1999**, *45*, 423.
[63] S. J. An, J. Li, C. Daniel, D. Mohanty, S. Nagpure, D. L. Wood, *Carbon* **2016**, *105*, 52.
[64] Z.-C. Wang, J. Xu, W.-H. Yao, Y.-W. Yao, Y. Yang, *ECS Trans.* **2012**, *41*, 29.
[65] R. Mogi, M. Inaba, S.-K. Jeong, Y. Iriyama, T. Abe, Z. Ogumi, *J. Electrochem. Soc.* **2002**, *149*, A1578.
[66] O. Borodin, M. Olguin, C. E. Spear, K. W. Leiter, J. Knap, *Nanotechnology* **2015**, *26*, 354003.
[67] J. Liu, Z. Chen, S. Busking, K. Amine, *Electrochem. Commun.* **2007**, *9*, 475.
[68] L. Xia, S. Lee, Y. Jiang, Y. Xia, G. Z. Chen, Z. Liu, *ACS Omega* **2017**, *2*, 8741.
[69] B. Lee, E. Paek, D. Mitlin, S. W. Lee, *Chem. Rev.* **2019**, *119*, 5416.
[70] Q. Lu, A. Yang, A. Omar, Q. Ma, F. Tietz, O. Guillon, D. Mikhailova, *Energy Technol.* **2022**, *10*, 2200149.
[71] F. Li, R. Liu, J. Liu, H. Li, *Adv. Funct. Mater.* **2023**, *33*, 2300602.
[72] K. Xu, A. v Cresce, U. Lee, *Langmuir* **2010**, *26*, 11538.
[73] A. Ponrouch, A. R. Goñi, M. R. Palacín, *Electrochem. Commun.* **2013**, *27*, 85.
[74] J. Fondard, E. Irisarri, C. Courrèges, M. R. Palacin, A. Ponrouch, R. Dedryvère, *J. Electrochem. Soc.* **2020**, *167*, 070526.

Manuscript received: December 11, 2024
Revised manuscript received: December 16, 2024
Version of record online: ■■, ■■

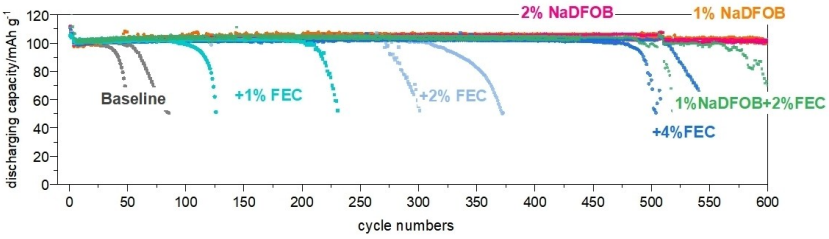

Improve of NaDFOB additivated electrolytes in case of sodium ion based half cells compared to FEC-containing electrolytes. Baseline electrolyte is $NaPF_6$ in EC/PC for all different formulations. Since the electrolyte containing NaDFOB significantly improves the half-cells and does not impair the full cells (unlike FEC, for example), this additive can be considered as a standard additive.

*Dr. Z. Wang, Dr. A. Hofmann**